Polímeros
ISSN 1678-5169 (Online)

https://doi.org/10.1590/0104-1428.20230103

ORIGINAL ARTICLE

Development by extrusion of composite films based on Poly(Lactic Acid)/Babassu Mesocarp Flour

Lucas Rafael Carneiro da Silva[1]*, Railha Antunes de França[2], Raquel do Nascimento Silva[2], Tatianny Soares Alves[2], Renata Barbosa[2], Alessandro de Oliveira Rios[3] and Ruth Marlene Campomanes Santana[1]

[1] Programa de Pós-graduação em Engenharia de Minas, Metalúrgica e de Materiais, Universidade Federal do Rio Grande do Sul – UFRGS, Porto Alegre, RS, Brasil

[2] Programa de Pós-graduação em Ciência e Engenharia dos Materiais, Universidade Federal do Piauí – UFPI, Teresina, PI, Brasil

[3] Programa de Pós-graduação em Ciência e Tecnologia de Alimentos, Universidade Federal do Rio Grande do Sul – UFRGS, Porto Alegre, RS, Brasil

**lr.rafaelcarneiro@gmail.com*

Abstract

The objective of this manuscript was to investigate the influence of different Babassu Mesocarp Flour (BMF) contents (3, 5, 8, and 10% by weight) on the physical and surface properties of the Poly(Lactic Acid) (PLA) matrix. For this purpose, composite films were produced through flat-die extrusion processing. Visual analysis showed that the films were successfully produced by this processing method and exhibited good handling. The physical properties of the films varied as follows: width (16.41–20.38 cm), thickness (0.14–0.24 mm), apparent density (0.78–1.07 g/cm^3), and grammage (168.34–255.31 g/m^2). Through optical microscopy, good distribution and dispersion of the particles were observed despite the presence of some agglomerates. The film surface became rough due to the incorporated flour content, which influenced the contact angle result. The combination of PLA/BMF for producing composite films has technological potential, enabling the valorization of an industrial by-product and preserving the environment.

Keywords: *Babassu Mesocarp Flour, composite films, flat-die extrusion, packaging, Poly(Lactic Acid).*

How to cite: Silva, L. R. C., França, R. A., Silva, R. N., Alves, T. S., Barbosa, R., Rios, A. O., & Santana, R. M. C. (2024). Development by extrusion of composite films based on Poly(Lactic Acid)/Babassu Mesocarp Flour. *Polímeros: Ciência e Tecnologia*, *34*(1), e20240009. https://doi.org/10.1590/0104-1428.20230103

1. Introduction

Over the years, polymer materials, commonly known as "plastics", have dominated the packaging industry, mainly those of petrochemical and non-biodegradable origin. This industry still widely uses plastics to produce short-term food packaging (single-use/disposable)[1]. It is crucial that the packaging produced can protect the packaged food, as its inefficiency results in the waste of resources and environmental impacts caused by improper disposal[2]. According to the 2021 United Nations Environment Programme (UNEP) report, plastic accounts for 85% of marine litter[3].

Alternative solutions to these environmental problems have been proposed to reduce the accumulation of non-biodegradable plastics in the environment. One of these alternatives is using plastics that combine renewable origin and biodegradable nature (biopolymers) to develop ecologically correct packaging, making it possible to meet the requirements of a more sustainable circular economy[4]. Among the available options, Poly(Lactic Acid) (PLA), a linear aliphatic polyester, is prominent in replacing conventional plastics and has aroused growing academic and industrial interest[5].

However, due to the relatively high polymer cost, producing a polymer film consisting only of PLA applied as a packaging material still needs to be economically feasible[6]. One promising option to minimize the cost of the final products based on PLA is to incorporate a fraction of another material into the polymer[7,8]. The ecological character of PLA must not be drastically affected; therefore, the incorporated material should also be environmentally friendly (bio-reinforcement).

From this perspective, incorporating industrial by-products is an ecological, promising, economic, and advantageous approach. Babassu Mesocarp Flour (BMF) is an excellent alternative, a by-product of the babassu oil extraction industry. The use of these materials helps to reduce the waste of resources, in addition to presenting exciting opportunities for innovation. The babassu palm (*Orbignya phalerata*, this species is the most common) is native to countries in South America, mainly in the Northeast and North of Brazil, being found in smaller proportions in Bolivia, Colombia, and Suriname. In Brazil, the central area of occurrence of

babassu is located in a transition zone between the tropical forests of the Amazon basin and the semi-arid region[9,10].

Based on the above, this manuscript aimed to investigate the physical (width, thickness, density, and grammage) and surface properties (optical microscopy, optical profilometry, and contact angle) of PLA/BMF-based films, as they directly influence the choice of a food model for subsequent film application. The films were produced by flat-die extrusion under laboratory conditions. Flat-die extrusion is highly efficient, allowing continuous film production quickly and economically with minimal downtime. It is a safe and ecological process, producing less waste than other production alternatives.

2. Materials and Methods

2.1 Materials

The polymer used was PLA, marketed under Ingeo™ Biopolymer 4043D (NatureWorks, Minnesota, USA). PLA exhibits the following properties: Density = 1.24 g/cm^3, Fluidity Index = 6 g/10 min (210 °C, 2.16 kg), and Melting Temperature (T_m) = 145–160 °C. The bio-reinforcement used was BMF obtained by grinding babassu mesocarp as part of the full use of babassu coconut (Florestas Brasileiras S.A., Itapecuru-Mirim, Maranhão, Brazil). Different techniques in our previous manuscript characterized BMF[11].

2.2 Masterbatch production based on PLA/BMF

The PLA and BMF were dried at 60 °C for 24 h in an oven with air circulation and renewal (De Leo, Porto Alegre, Brazil). The concentrates (masterbatch) were prepared in the proportion of 50% PLA and 50% BMF. That is, 25 g of each material was used (50 g). The equipment used was an Internal Mixer (Model HAAKE™ Rheomix 600 OS, Thermo Scientific) operating at 160 °C with a rotation speed of roller-type rotors of 60 rpm. PLA pellets were fed into the equipment at the beginning of the processing. After 4 min, the internal mixer was fed with BMF without interrupting the process until the total time was 8 min. The masterbatch obtained was ground in a Knife Mill (PROJEMAQ Engenharia, Brazil).

2.3 Preparation of PLA/BMF film formulations

The ground material was dried at 60 °C for 24 h in an oven (Model SL-100, Solab, Brazil). Subsequently, the material was diluted in virgin PLA resin in adequate amounts to produce formulations with 3, 5, 8, and 10% by weight of BMF. The BMF contents used in this manuscript were based on the literature regarding producing films from composites[12,13]. The dilution was carried out in a Single-Screw Extruder (screw diameter = 16 mm; L/D ratio = 26), Model AX-16 by AX Plásticos, with a temperature profile of 145, 155, and 170 °C and with a screw speed of 50 rpm. The virgin PLA pellets were dried and processed with the same parameters. Table 1 presents the formulations and their respective identification code.

2.4 Processing of films by flat-die extrusion

Figure 1 shows the extruder with the flat-die (width = 22 cm) and some images captured during film processing. The previous topic described processing temperatures and screw speed.

Table 2 presents the parameters used for film processing. After the end of the processing, the films were stored in Low-Density Polyethylene (LDPE) hermetic zip-lock bags (35 × 45 cm).

Table 1. PLA/BMF-based film formulations and their identification code.

Film Formulations	Content (%)		Identification Code
	PLA	BMF	
Neat PLA	100	0	Neat PLA
PLA/3%BMF	97	3	P/3F
PLA/5%BMF	95	5	P/5F
PLA/8%BMF	92	8	P/8F
PLA/10%BMF	90	10	P/10F

Caption: P = PLA; F = Flour.

Figure 1. Flat-die extrusion equipment and images captured during film processing.

Table 2. Processing parameters used for film production.

Film Formulations	Parameters – Chill Rolls (rpm)			
	Cooling Roller 1	Cooling Roller 2	Puller Roller	Film Winder
Neat PLA	1.5	3.9	3.0	6.8
PLA/3%BMF	1.5	2.0	3.0	6.9
PLA/5%BMF	1.5	2.0	3.0	6.9
PLA/8%BMF	1.5	2.0	3.0	6.9
PLA/10%BMF	1.5	2.0	3.0	6.9

2.5 Characterization of composite films

The physical aspect of the films was evaluated through visual and tactile observations to elucidate the influence of flat-die extrusion processing and the incorporated BMF content. Surface irregularities (macroscopic scale) were also investigated for discussion purposes. The images of the films were captured using a *Samsung Galaxy M51* (64 megapixels).

The average width of the films was determined based on twenty measurements using a graduated ruler. Each film reel was unwound, and measurements were taken at different lengths. The average width value was used to calculate the Transverse Ratio (TR) (Equation 1):

$$TR = \frac{W_{film}}{W_{flat-die}} \quad (1)$$

Where: W_{FILM} is the average width of the film (cm), and $W_{FLAT\text{-}DIE}$ is the width of the flat-die used in the extrusion, corresponding to 22 cm. The closer the TR value is to 1, the closer the film width is to that of the flat-die.

The thickness of the samples was determined using a thickness gauge with a graduation of 0.01 mm and an accuracy of ±0.02 mm (Model 130.125, DIGIMESS, São Paulo, Brazil). Six film samples for each formulation, each 3.0 × 3.0 cm in size, were used for the analysis. The thickness was measured at ten points on the sample: two in the central part and eight in the perimeter.

The apparent density of the film was calculated directly from the ratio between mass and volume by Equation 2. The sample dimension was 1.7 × 1.7 cm, and the thickness was measured with a thickness gauge (Model M-73010, Mainard, São Paulo, Brazil) in the central part of the sample. The final density value was presented as the average of six replicates.

$$\rho = \frac{m}{Ax\delta} \quad (2)$$

where: m is the mass of the sample (g), A is the area of the sample (2.89 cm^2), δ is the thickness of the sample (cm), and ρ is the film density expressed in g/cm^3.

The grammage of the film samples was determined as the average ratio between the mass and area of six samples according to Equation 3:

$$G = \frac{m}{A} \quad (3)$$

where: m is the mass of the sample (g), A is the sample area (0.000289 m^2), and G is the average grammage of the film (g/m^2).

The film samples were analyzed in a Binocular Optical Microscope (Model DM500, Leica Microsystems) under the following conditions: transmission mode, ICC50 E capture camera, 40x magnification, and 500 µm scale. The sample was taken from a region between the film perimeter and the center.

The 3D Optical Profilometry technique (Model ContourGT-K, Bruker) investigated the surface topography and quantitative parameters, such as average roughness (R_A), maximum peak height (R_P), and maximum valley depth (R_V). Topographic images (2D and 3D) were obtained from a film sample measuring 0.9 x 1.3 mm, and the parameters were expressed in µm. The "Vision6" software was used for data acquisition.

Contact angle measurements (sessile drop method) were performed using a Drop Shape Analyzer-DSA100 (KRÜSS Scientific, Germany) to analyze the samples surface wettability. This method gently deposited a deionized water droplet onto the sample surface using a micro syringe at room temperature and humidity. The "DSA4" software calculated the contact angle based on the droplet image captured ~5 s after the droplet was deposited. The final value is the average of twenty measurements for each film formulation.

3. Results and Discussions

3.1 Visual evaluation

Figure 2 presents the film reels produced to explain the efficiency of the flat-die extrusion processing and report the observed surface irregularities.

All films were successfully produced using the flat-die extrusion. It is vital to make it clear that the films were not free of surface irregularities and, therefore, tiny pores were observed in different regions of the film. The surface lines from the melt flow were best visualized on the PLA film surface. This type of processing is highly productive, so the films produced are long and wide. The parameters must be set correctly to prevent the films from tearing during processing. Here, the parameters used allowed the production of continuous films. The films produced did not show brittle behavior when handled, which allowed them to be rolled up during processing. The composite films were easier to roll up as the BMF content increased, possibly due to obtaining a thinner thickness for a higher flour content. The PLA-based film showed high brightness, transparency, and good handling, and the composite films were opaque (Figure 3).

3.2 Width inspection

One of the main tasks of a flat-die is to distribute the molten polymer to the desired width and thickness and

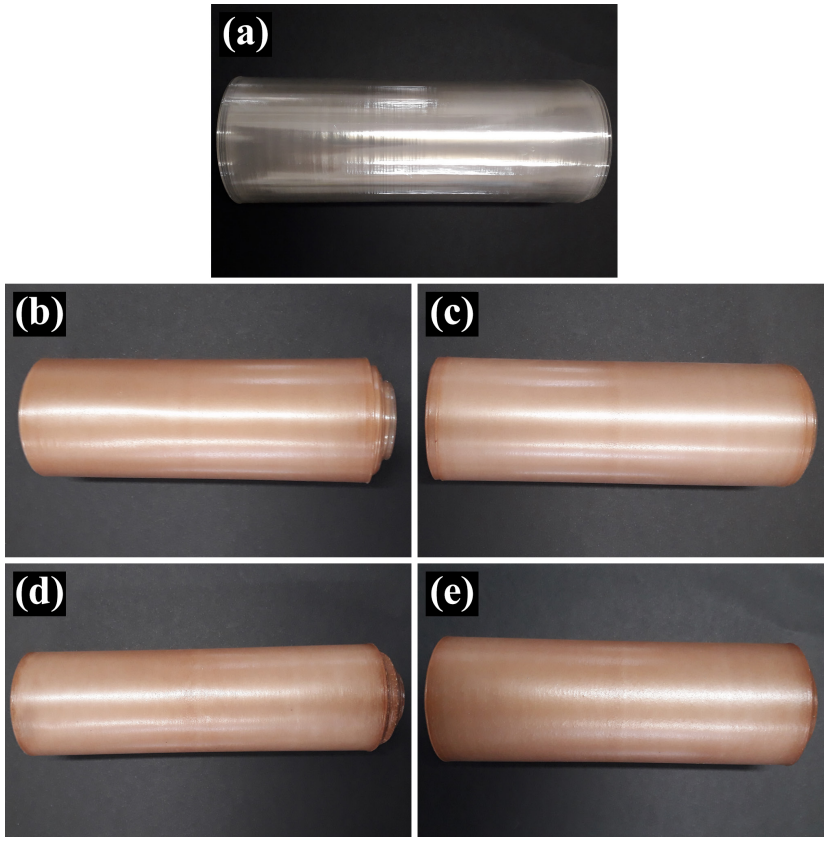

Figure 2. Film reels: (a) Neat PLA, (b) P/3F, (c) P/5F, (d) P/8F, and (e) P/10F.

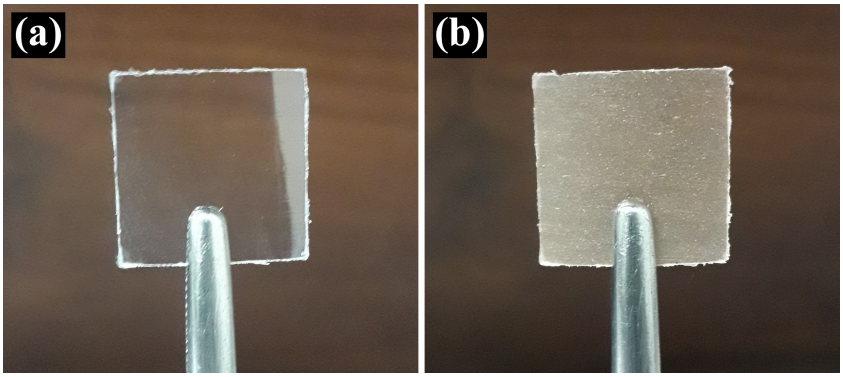

Figure 3. Digital photograph of neat PLA and PLA/BMF (8% by weight) film samples highlighting: (a) transparency and (b) opacity, respectively.

develop a uniform flow pattern[14]. Thus, as shown in Figure 4, the influence of BMF on the width of composite films was investigated.

As shown in Figure 4, all films produced have a smaller width than the width of the flat-die. The results showed that the film based on neat PLA had the greatest width, as there was no component in the film formulation that could restrict the flow of molten material and considerably reduce the width in processing, showing a reduction of 7.36%. With the incorporation of BMF in different contents to the PLA matrix, it was observed that the width was even more reduced, resulting in 25.41 (P/3F), 21.41 (P/5F), 12.91 (P/8F), and 11.59% (P/10F). Incorporating BMF into PLA may have limited its polymer chain mobility, and the composite film width was smaller due to the reduced melt flow.

A distinct reason that justifies reducing the width of all films is shown in Figure 5a. The molten material exiting the flat-die is directed along the edge of the film because the equipment rollers pull the film away from the flat-die. Consequently, the width of the film was reduced due to this

stretching. During film processing, stretching is inevitable as the extruded material is pulled along the processing flow direction (machine direction). This phenomenon of reducing the width of the film is known as "neck-in"; therefore, it is recommended that the width of the flat-die be greater than that of the final product[15].

Another interpretation would be that the BMF content for the composite films influenced the neck-in. As the film was pulled and rolled up at a certain speed during processing, a fraction of the BMF particles drifted toward the film edges (Figure 5b and 5c). Therefore, with lower particle content at the edges, the reduction in width was more pronounced, and with an increase in particle content, the width did not undergo significant reductions. However, it is essential to mention that the reduction of the film width by the flat-die makes the edges of the film thicker than the center of the film (edge bead)[16]. Composite films based on 3 and 5% by weight of BMF showed the thickest edges. Thus, the previously raised idea that the lower particle content on the edges could facilitate the width reduction may not have impacted the results. Thicker edges would make it more challenging to reduce the width, which leads to the assumption that the reduction in width due to the neck-in acted more relevantly. The TR results were 0.93 (Neat PLA), 0.75 (P/3F), 0.79 (P/5F), 0.87 (P/8F), and 0.88 (P/10F).

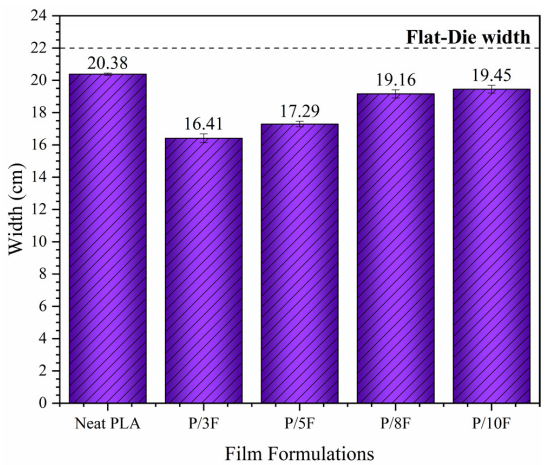

Figure 4. Average width of the films produced compared to flat-die width.

3.3 Thickness measurements

Thickness is an essential characteristic of polymer films used in food packaging. Figure 6 shows the average thickness of the films produced.

In general, the average thickness of the films varied between 0.14–0.24 mm, within the thickness range explained by Barlow and Morgan[17]. According to the authors, the thickness of the films applied to food packaging varies between 10–250 µm (0.01–0.25 mm) depending on the resistance, durability, and barrier function determined by the application. All films incorporating BMF were thicker than the neat PLA film, and this increase in thickness was due to the incorporated solid particles. The incorporation of BMF increased to 71 (P/3F), 57 (P/5F), 50 (P/8F), and 43% (P/10F), showing that film composition substantially affects thickness. The difference between each formulation may be due to differences in flour particle size, melt viscosity, and interactions and structural changes that establish different rearrangements during the film processing stage, influencing the thickness.

On the other hand, it was observed in the literature that the justification for a smaller thickness for some film formulations is due to a compact molecular structure[18]. For films produced by flat-die extrusion, it was reported in the literature that the cooling roller rotational speed must be adjusted to be high enough to make the films thinner[19]. However, it is necessary to pay attention to this consideration, as the high rotation speeds of the rollers can make it difficult for the continuous formation of the film when it exits through the die slit. Consequently, films can tear or show many irregularities.

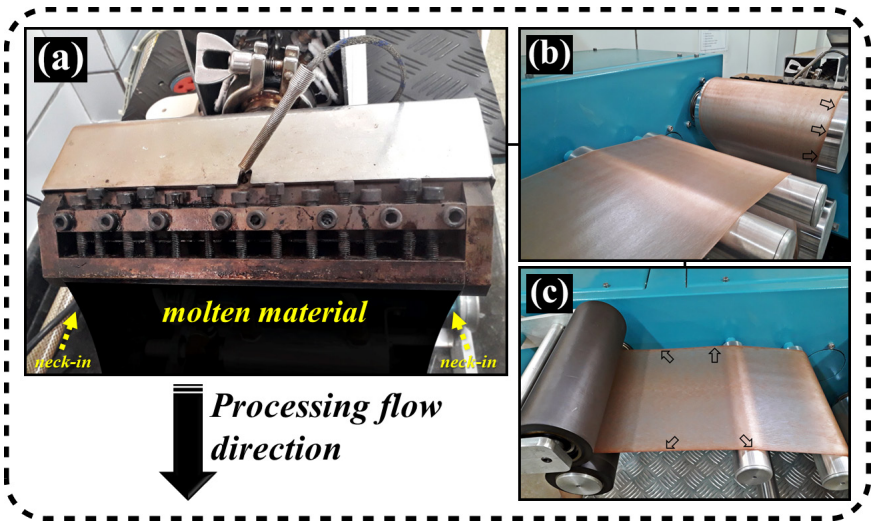

Figure 5. Scheme showing: (a) neck-in and (b–c) film edge with flour particles.

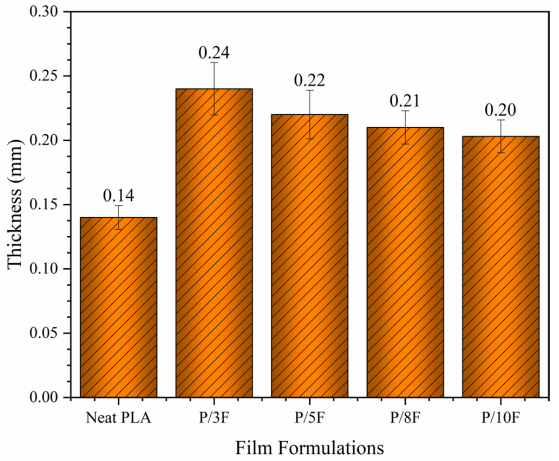

Figure 6. Average thickness of the films produced by flat-die extrusion.

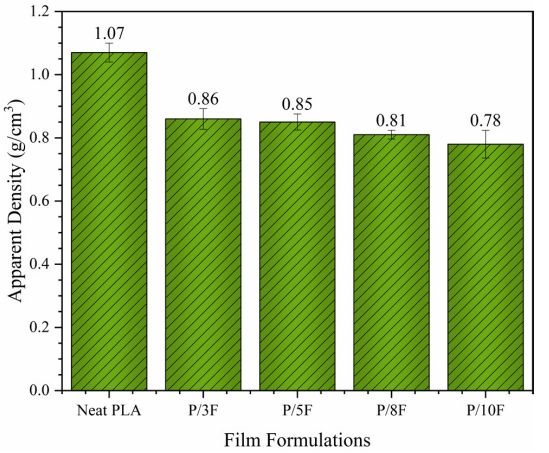

Figure 7. Average apparent density value determined for the films.

3.4 Apparent density (ρ)

The density measures the mass amount in a given volume. Thus, the density of the films produced was determined, and the result obtained is shown in Figure 7.

The film produced based on neat PLA had a density of 1.07 ± 0.030 g/cm^3, the highest value obtained concerning the density of films incorporated with BMF. The incorporation of BMF into the PLA caused a reduction in film density as the BMF content increased, resulting in a density < 1.0 g/cm^3 for all composite films. The flour possibly acted, in this case, as a filler material, causing the particles to occupy space within the polymer matrix, increasing its volume without adding a significant mass amount. In percentage terms, the reduction suffered was 19.63 (P/3F), 20.56 (P/5F), 24.30 (P/8F), and 27.10% (P/10F) due to the low density of BMF particles. This variation observed in the density of the composite films and associated with the BMF content may also be associated with the level of porosity in the film structure[20]. The lower density of composite films makes them attractive materials, mainly for applications related to lightness and easy handling, such as food packaging.

3.5 Grammage

Grammage is an analysis widely used to compare papers of different types, such as common paper and cardboard, to investigate the influence of a coating on the paper applied as a packaging material. Thus, as shown in Figure 8, the grammage was determined to understand how the BMF particles interfere with this property.

The grammage of the neat PLA film was 168.34 ± 4.510 g/m^2, the lowest value among the films produced. Incorporating BMF increased the film grammage for all incorporated contents into PLA. However, the grammage linearly reduced with the increase in flour content, namely: 255.31 ± 9.763 (P/3F) > 214.30 ± 5.346 (P/5F) > 189.45 ± 5.342 (P/8F) > 177.80 ± 7.322 g/m^2 (P/10F). This reduction in grammage with increasing flour content occurred because the particles decreased the amount of polymer material in the film. The increase in the grammage of the composite films

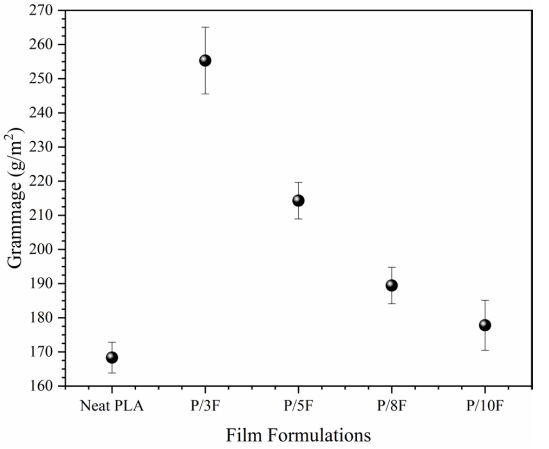

Figure 8. Average grammage determined for films.

may have some relationship with filling the free volume "cavities" in the PLA with BMF particles. The incorporated particles can change the free volume[21]. The variation in grammage between the different formulations may be due to differences in composition, structure, thickness, and pore volume[22].

3.6 Optical Microscopy (OM)

The OM technique can investigate the distribution and dispersion of the material incorporated in the polymer matrix. Thus, in Figure 9, micrographs of the film surface are presented, which allowed the observation of the distribution and dispersion of the BMF incorporated into the PLA.

The micrograph of the neat PLA film showed a relatively homogeneous surface due to the absence of BMF particles (Figure 9a). In contrast, particles of different sizes on the surface of composite films were randomly distributed in the polymer matrix, representing a heterogeneous surface. The increase in BMF content caused the appearance of small agglomerates of particles, better visualized in Figures 9d and 9e, which is inevitable, as the particles do not melt and poor dispersion

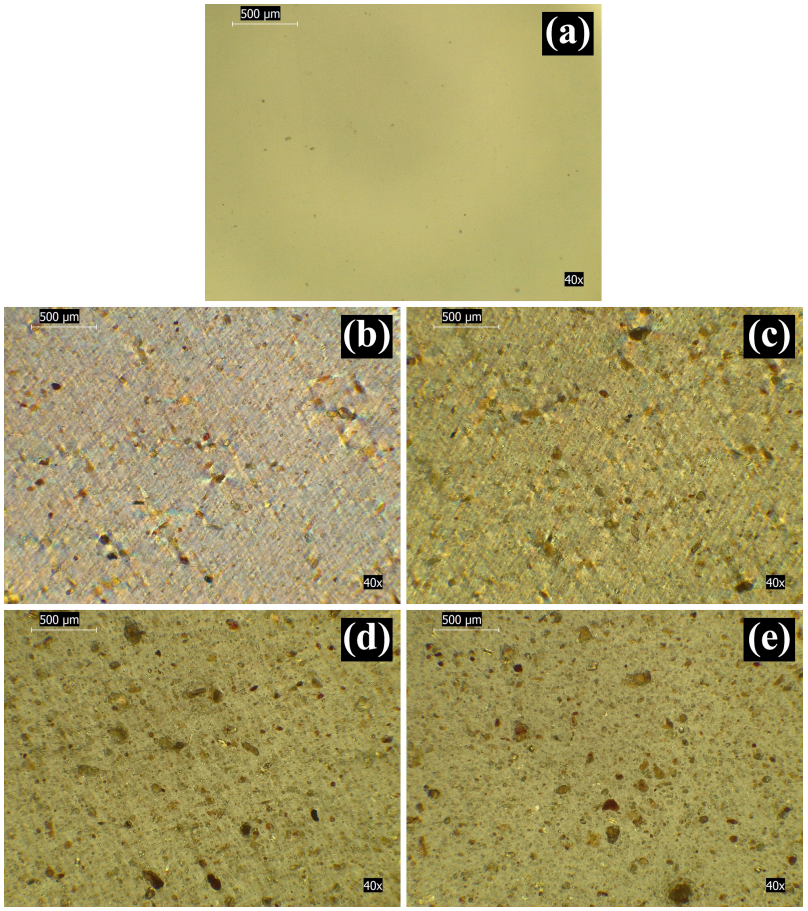

Figure 9. Optical micrographs: (a) Neat PLA, (b) P/3F, (c) P/5F, (d) P/8F, and (e) P/10F.

was present at some locations of the film. The observation of agglomerates is more visible at higher contents of BMF due to the increase in particle density, which results in the interaction between fine particles (cohesive forces) and, consequently, in forming these agglomerates. The minimal presence of large agglomerates in the films was mainly due to the mixing step between the PLA and the BMF in the internal mixer to produce the masterbatch.

3.7 Optical profilometry

Table 3 presents the topographic images in 2D and 3D (qualitative parameters) obtained by optical profilometry of the film surfaces. Table 4 presents the values of the quantitative parameters (R_A, R_P, and R_V) obtained.

In general, all films presented a rough surface since, at first, the processing by flat-die extrusion influences this aspect. Surface roughness imposed by processing may be due to friction between the film, the flat-die, and the equipment rollers. For all images (2D and 3D), brightness and contrast correspond to the color palette next to the image[23]. The lowest height level in all cases refers to dark blue (valleys). In contrast, the highest level is given in red (peaks), suggesting that the film surface is asymmetrical and irregular. The neat PLA film showed the "smoothest" surface. Differently, for composite films, it was observed that changes in roughness parameters were a function of flour content, with numerous randomly distributed valleys and peaks. The topographical differences between the composite films may demonstrate that the particles were not dispersed entirely in the polymer matrix (Figure 9).

The roughness parameters presented in Table 4 refer only to the profile in the vertical direction (valleys and peaks) and, therefore, do not provide information on the inclinations and shapes of the roughness nor the amount of existing roughness on the surface[24]. The fact that the neat PLA film presented a slightly higher R_A value than the P/3F and P/5F film was due to the processing. This same film exhibited several surface lines due to the molten material flow during processing, which was most evident in its 3D topographic image. It is also worth mentioning that any impurity on the surface can influence the roughness parameters since no particles were incorporated intentionally for neat PLA film. Valleys are also called depressions associated with surface pores[25]. The dark regions observed in the 2D images can be related to these pores.

3.8 Contact angle (θ)

The contact angle characterizes the degree of wettability and can designate the hydrophilic or hydrophobic nature of the film surface. Generally, a contact angle less than 90° refers

Table 3. Optical profilometry images showing the different topographic profiles.

Film Formulations	Topographic Images	
	2D	3D
Neat PLA	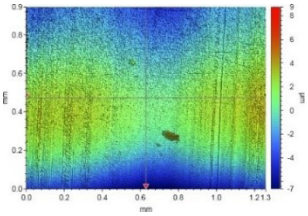	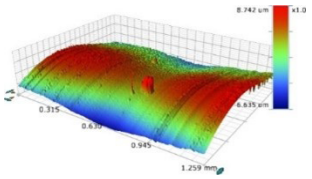
P/3F	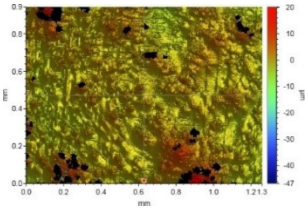	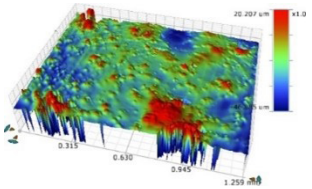
P/5F	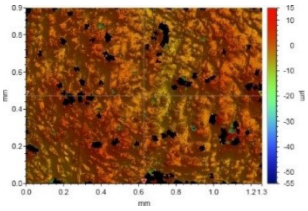	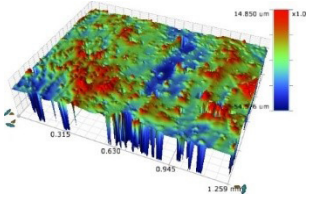
P/8F	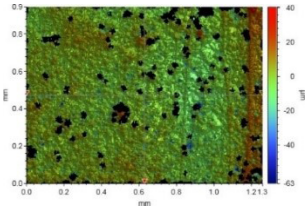	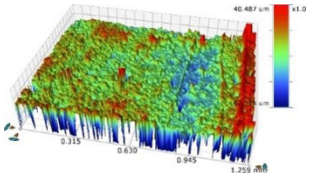
P/10F	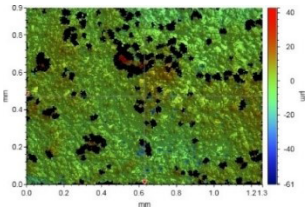	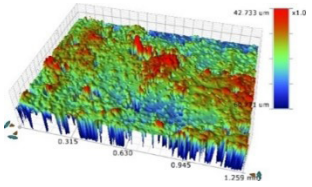

to a hydrophilic surface, while greater than 90° represents a hydrophobic surface[26]. Average values and representative images of the water droplet are shown in Table 5.

The contact angle of the neat PLA-based film was 80.76°, resulting in a hydrophilic surface. This result may be due to the hydroxyl and carbonyl groups (polar) present in the chemical structure of PLA. The incorporation of BMF slightly reduced the contact angle from 80.76° to values below 80° for composite films. The smaller the contact angle, the greater the surface affinity for the reference liquid, resulting in greater wettability. The angle reduction resulted in greater surface hydrophilicity of the composite films, related to the greater availability of hydroxyl groups from the starch in BMF. These groups can interact with water molecules on the film surface and reduce the contact angle.

Table 4. Surface roughness parameters values of the films produced.

Film Formulations	Roughness Parameters (µm)		
	R_A	R_P	R_V
Neat PLA	1.76	8.74	-6.64
P/3F	1.45	20.21	-46.89
P/5F	1.49	14.85	-54.58
P/8F	4.92	40.49	-62.52
P/10F	3.84	42.73	-60.77

Caption: R_A = average roughness; R_P = maximum peak height; R_V = maximum valley depth.

Although the composite films exhibited a hydrophilic character, the droplet remained stable on the film surface

Table 5. Contact angle value of the films and the representative image of the water droplet.

Film Formulations	Contact Angle (°)	
	Average Value	Water Droplet Image
Neat PLA	80.76 ± 2.64	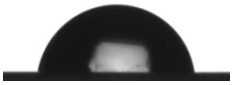
P/3F	79.40 ± 2.42	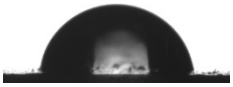
P/5F	76.73 ± 3.24	
P/8F	79.62 ± 1.86	
P/10F	78.22 ± 1.70	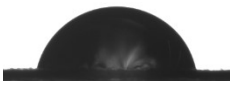

Data were expressed as mean ± standard deviation (n = 20).

without changes during the analysis, showing that the films are not hydrophilic enough to absorb the droplet. The images of the droplet did not reveal significant visual differences in its size, indicating minimal water absorption by the samples. Despite the surface roughness substantially influencing the contact angle value, there was no linear relationship between the analysis of the contact angle and the roughness results (Table 4). A less rough surface, that is, more homogeneous, provides a better droplet distribution on the surface, reducing the contact angle and, consequently, greater wettability. In contrast, the angle is greater for a rougher surface (more heterogeneous). Table 5 shows that the contact angle did not decrease linearly with the increase in flour content. This understanding is due to the surface heterogeneity caused by roughness that influences different contact angles in different parts of the same solid surface.

The result of the contact angle suggests that the application of the films should be directed, in principle, to low/intermediate moisture products, aiming at the structural integrity of the films. One of the essential properties of materials applied in packaging is the surface polarity, reflecting the interaction of the surface with the printing ink. So, higher polarity results in a more hydrophilic surface and better printability[27]. This discussion is relevant because consumers consider the aesthetic presentation of the packaged product, which may be associated with the label printed on the package.

4. Conclusions

This manuscript highlighted a viable strategy to enhance and add value to BMF, an industrial by-product, through its incorporation into the PLA polymer matrix. The effect of different flour contents was investigated on the physical and surface properties of composite films produced by flat-die extrusion. The processing was satisfactory in producing continuous films, although some surface irregularities were observed. No chemical solvents were used, contributing to an environmentally friendly production step. The research focused on the use of by-products incorporated into a polymer matrix for the development of composite materials is constantly growing, both in academia and industry, as they are materials that have many ecological advantages. Choosing the right package with the proper physical and surface properties is essential to ensure the safety and quality of packaged food. The films produced are good candidates for a potential application as a food packaging material, as the results showed interesting perspectives for such an application.

5. Author's Contribution

- **Conceptualization –** Lucas Rafael Carneiro da Silva; Ruth Marlene Campomanes Santana.
- **Data curation –** Lucas Rafael Carneiro da Silva.
- **Formal analysis –** Lucas Rafael Carneiro da Silva.
- **Funding acquisition –** NA.
- **Investigation –** Lucas Rafael Carneiro da Silva; Ruth Marlene Campomanes Santana.
- **Methodology –** Lucas Rafael Carneiro da Silva; Railha Antunes de França; Raquel do Nascimento Silva; Ruth Marlene Campomanes Santana.
- **Project administration –** Ruth Marlene Campomanes Santana.
- **Resources –** Ruth Marlene Campomanes Santana; Renata Barbosa; Tatianny Soares Alves.
- **Software –** NA.
- **Supervision –** Ruth Marlene Campomanes Santana; Alessandro de Oliveira Rios.
- **Validation –** Lucas Rafael Carneiro da Silva; Ruth Marlene Campomanes Santana.
- **Visualization –** Lucas Rafael Carneiro da Silva.
- **Writing – original draft –** Lucas Rafael Carneiro da Silva.
- **Writing – review & editing –** Lucas Rafael Carneiro da Silva; Ruth Marlene Campomanes Santana; Alessandro de Oliveira Rios.

6. Acknowledgements

The authors want to acknowledge the Federal University of Rio Grande do Sul (UFRGS), Postgraduate Program in Mining, Metallurgical and Materials Engineering (PPGE3M), and National Council for Scientific and Technological Development (CNPq) [process number: 140519/2021-1]. We would also like to acknowledge the support of Daniel Eduardo Weibel, PhD, and Alexandra Aponte, scholarship holder (LAMAS/UFRGS).

7. References

1. Vidal, O. L., Santos, M. C. B., Batista, A. P., Andrigo, F. F., Baréa, B., Lecomte, J., Figueroa-Espinoza, M. C., Gontard, N., Villeneuve, P., Guillard, V., Rezende, C. M., Bourlieu-Lacanal, C., & Ferreira, M. S. L. (2022). Active packaging films containing antioxidant extracts from green coffee oil by-products to prevent lipid oxidation. *Journal of Food Engineering*, *312*, 110744. http://dx.doi.org/10.1016/j.jfoodeng.2021.110744.

2. Flores-Silva, P. C., Hernández-Hernández, E., Sifuentes-Nieves, I., Lara-Sánchez, J. F., Ledezma-Pérez, A. S., Alvarado-Canché, C. N., & Ramírez-Vargas, E. (2023). Active mono-material films from natural and post-consumer recycled polymers with essential oils for food packaging applications. *Journal of Polymers and the Environment*, *31*(12), 5198-5209. http://dx.doi.org/10.1007/s10924-023-02943-6.
3. United Nations Environment Programme. (2021). *Annual Report 2021*. Kenya: UNEP. Retrieved in 2023, December 21, from https://www.unep.org/annualreport/2021/index.php
4. Chen, C., Chen, W., Dai, F., Yang, F., & Xie, J. (2022). Development of packaging films with gas selective permeability based on Poly(butylene Adipate-co-terephthalate)/Poly(butylene Succinate) and its application in the storage of white mushroom (*Agaricus bisporus*). *Food and Bioprocess Technology*, *15*(6), 1268-1283. http://dx.doi.org/10.1007/s11947-022-02794-4.
5. Raza, Z. A., & Anwar, F. (2018). Fabrication of poly(lactic acid) incorporated chitosan nanocomposites for enhanced functional polyester fabric. *Polímeros: Ciência e Tecnologia*, *28*(2), 120-12. http://dx.doi.org/10.1590/0104-1428.11216.
6. Bhagia, S., Bornani, K., Agrawal, R., Satlewal, A., Ďurkovič, J., Lagaňa, R., Bhagia, M., Yoo, C. G., Zhao, X., Kunc, V., Pu, Y., Ozcan, S., & Ragauskas, A. J. (2021). Critical review of FDM 3D printing of PLA biocomposites filled with biomass resources, characterization, biodegradability, upcycling and opportunities for biorefineries. *Applied Materials Today*, *24*, 101078. http://dx.doi.org/10.1016/j.apmt.2021.101078.
7. Barbosa, J. D. V., Azevedo, J. B., Araújo, E. M., Machado, B. A. S., Hodel, K. V. S., & Mélo, T. J. A. (2019). Bionanocomposites of PLA/PBAT/organophilic clay: preparation and characterization. *Polímeros: Ciência e Tecnologia*, *29*(3), e2019045. http://dx.doi.org/10.1590/0104-1428.09018.
8. Raj, S. S., Kannan, T. K., & Rajasekar, R. (2020). Influence of prosopis juliflora wood flour in poly lactic acid – developing a novel bio-wood plastic composite. *Polímeros: Ciência e Tecnologia*, *30*(1), e2020012. http://dx.doi.org/10.1590/0104-1428.00120.
9. Protásio, T. P., Trugilho, P. F., César, A. A. S., Napoli, A., Melo, I. C. N. A., & Silva, M. G. (2014). Babassu nut residues: potential for bioenergy use in the North and Northeast of Brazil. *SpringerPlus*, *3*(1), 124. http://dx.doi.org/10.1186/2193-1801-3-124. PMid:24741469.
10. Yapuchura, E. R., Tartaglia, R. S., Cunha, A. G., Freitas, J. C. C., & Emmerich, F. G. (2019). Observation of the transformation of silica phytoliths into SiC and SiO_2 particles in biomass-derived carbons by using SEM/EDS, Raman spectroscopy, and XRD. *Journal of Materials Science*, *54*(5), 3761-3777. http://dx.doi.org/10.1007/s10853-018-3130-6.
11. Silva, L. R. C., Alves, T. S., Barbosa, R., Dal Pont Morisso, F., Rios, A. O., & Santana, R. M. C. (2023). Characterization of babassu mesocarp flour as potential bio-reinforcement for Poly (Lactic Acid). *Journal of Food Industry*, *7*(1), 24-53. http://dx.doi.org/10.5296/jfi.v7i1.21066.
12. Bernhardt, D. C., Pérez, C. D., Fissore, E. N., De'Nobili, M. D., & Rojas, A. M. (2017). Pectin-based composite film: effect of corn husk fiber concentration on their properties. *Carbohydrate Polymers*, *164*, 13-22. http://dx.doi.org/10.1016/j.carbpol.2017.01.031. PMid:28325309.
13. Cao, C., Wang, Y., Zheng, S., Zhang, J., Li, W., Li, B., Guo, R., & Yu, J. (2020). Poly (butylene adipate-*co*-terephthalate)/titanium dioxide/silver composite biofilms for food packaging application. *Lebensmittel-Wissenschaft + Technologie*, *132*, 109874. http://dx.doi.org/10.1016/j.lwt.2020.109874.
14. Rosato, D. V., Rosato, D. V., & Rosato, M. V. (2004). *Plastic product material and process selection handbook.* UK: Elsevier Advanced Technology. http://dx.doi.org/10.1016/B978-1-85617-431-2.X5000-2.
15. Giles, H. F., Jr., Mount, E. M., 3rd, & Wagner, J. R., Jr. (2004). *Extrusion: the definitive processing guide and handbook.* USA: William Andrew.
16. Dhadwal, R., Banik, S., Doshi, P., & Pol, H. (2017). Effect of viscoelastic relaxation modes on stability of extrusion film casting process modeled using multi-mode Phan-Thien-Tanner constitutive equation. *Applied Mathematical Modelling*, *47*, 487-500. http://dx.doi.org/10.1016/j.apm.2017.03.010.
17. Barlow, C. Y., & Morgan, D. C. (2013). Polymer film packaging for food: an environmental assessment. *Resources, Conservation and Recycling*, *78*, 74-80. http://dx.doi.org/10.1016/j.resconrec.2013.07.003.
18. Guimarães, B. M. R., Scatolino, M. V., Martins, M. A., Ferreira, S. R., Mendes, L. M., Lima, J. T., Guimarães, M., Jr., & Tonoli, G. H. D. (2022). Bio-based films/nanopapers from lignocellulosic wastes for production of added-value micro-/nanomaterials. *Environmental Science and Pollution Research International*, *29*(6), 8665-8683. http://dx.doi.org/10.1007/s11356-021-16203-4. PMid:34490567.
19. Bechert, M. (2020). Non-Newtonian effects on draw resonance in film casting. *Journal of Non-Newtonian Fluid Mechanics*, *279*, 104262. http://dx.doi.org/10.1016/j.jnnfm.2020.104262.
20. Ahmed, S., & Ikram, S. (2016). Chitosan and gelatin based biodegradable packaging films with UV-light protection. *Journal of Photochemistry and Photobiology. B, Biology*, *163*, 115-124. http://dx.doi.org/10.1016/j.jphotobiol.2016.08.023. PMid:27560490.
21. Harms, S., Rätzke, K., Faupel, F., Schneider, G. J., Willner, L., & Richter, D. (2010). Free volume of interphases in model nanocomposites studied by positron annihilation lifetime spectroscopy. *Macromolecules*, *43*(24), 10505-10511. http://dx.doi.org/10.1021/ma1022692.
22. Bilck, A. P., Grossmann, M. V. E., & Yamashita, F. (2010). Biodegradable mulch films for strawberry production. *Polymer Testing*, *29*(4), 471-476. http://dx.doi.org/10.1016/j.polymertesting.2010.02.007.
23. Albuquerque, M. D. F., Bastos, D. C., Ţălu, Ş., Matos, R. S., Pires, M. A., Salerno, M., Fonseca Filho, H. D., & Simão, R. A. (2022). Vapor barrier properties of cold plasma treated corn starch films. *Coatings*, *12*(7), 1006. http://dx.doi.org/10.3390/coatings12071006.
24. Bhushan, B. (2000). *Surface roughness analysis and measurement techniques.* In B. Bhushan (Ed.), *Modern tribology handbook* (pp. 79-150). USA: CRC Press. http://dx.doi.org/10.1201/9780849377877-10.
25. Waduge, R. N., Xu, S., & Seetharaman, K. (2010). Iodine absorption properties and its effect on the crystallinity of developing wheat starch granules. *Carbohydrate Polymers*, *82*(3), 786-794. http://dx.doi.org/10.1016/j.carbpol.2010.05.053.
26. Kasai, D., Chougale, R., Masti, S., Chalannavar, R., Malabadi, R. B., Gani, R., & Gouripur, G. (2019). An investigation into the influence of filler *piper nigrum* leaves extract on physicochemical and antimicrobial properties of Chitosan/Poly (Vinyl Alcohol) blend films. *Journal of Polymers and the Environment*, *27*(3), 472-488. http://dx.doi.org/10.1007/s10924-018-1353-x.
27. Esmaeili, M., Pircheraghi, G., Bagheri, R., & Altstädt, V. (2019). Poly(lactic acid)/coplasticized thermoplastic starch blend: effect of plasticizer migration on rheological and mechanical properties. *Polymers for Advanced Technologies*, *30*(4), 839-851. http://dx.doi.org/10.1002/pat.4517.

Received: Dec. 21, 2023
Revised: Jan. 29, 2024
Accepted: Feb. 05, 2024